



Published in final edited form as:

J Cell Mol Med. 2011 October ; 15(10): 2117–2129. doi:10.1111/j.1582-4934.2010.01241.x.

Therapeutic Effects of Human STRO-3-Selected Mesenchymal Precursor Cells and their Soluble Factors in Experimental Myocardial Ischemia

Fiona See, PhD^{1,2,*}, Tetsunori Seki, PhD², Peter J Psaltis, MBBS³, Hugo P Sondermeijer, MD, MS², Stan Gronthos, PhD³, Andrew CW Zannettino, PhD³, Klaas M Govaert², Michael D Schuster, MBA², Paul A Kurlansky, MD⁴, Darren J Kelly, PhD^{1,*}, Henry Krum, MBBS, PhD⁵, and Silviu Itescu, MBBS^{1,2}

¹ University of Melbourne, St Vincent's Hospital, Department of Medicine, Victoria, Australia

² Columbia University, Department of Surgery, New York, USA

³ Centre for Stem Cell Research, Department of Medicine, University of Adelaide, South Australia, Australia

⁴ Miami Heart Research Institute, Florida, USA

⁵ NHMRC CCRE in Therapeutics, Monash University, Alfred Hospital, Victoria, Australia

Abstract

Background—The STRO-3 antigen has previously been shown to identify a subset of adult human bone marrow (BM)-derived mesenchymal lineage precursors, which may have cardioprotective potential. We sought to characterize STRO-3⁺-immunoselected and culture-expanded mesenchymal precursor cells (MPCs) with respect to their biology and therapeutic potential in myocardial ischemia.

Methods and Results—Immunoselection of STRO-3⁺ MPCs enriched for fibroblastic colony forming units from unfractionated BM MNCs. Compared to mesenchymal stem cells conventionally isolated by plastic adherence, MPCs demonstrated increased proliferative capacity during culture-expansion, expressed higher levels of early “stem cell” markers and various proangiogenic and cardioprotective cytokines, and exhibited greater trilineage developmental efficiency. Intramyocardial injection of MPCs into a rat model of myocardial infarction (MI) promoted LV recovery and inhibited LV dilatation. These beneficial effects were associated with cardioprotective and proangiogenic effects at the tissue level, despite poor engraftment of cells. Treatment of MI rats with MPC-conditioned medium (CM) preserved LV function and dimensions, reduced myocyte apoptosis and fibrosis, and augmented neovascularization, involving both resident vascular cells and circulating endothelial progenitor cells (EPCs). Profiling of CM revealed various cardioprotective and proangiogenic factors, which had biological activity in cultures of myocytes, tissue-resident vascular cells and EPCs.

*Addresses for Correspondence: Fiona See, PhD, The Leon H. Charney Division of Cardiology, Cardiovascular Research Program, New York University Langone School of Medicine, 522 First Avenue, Smilow 8, New York, NY 10016, USA, Tel: +1.212.263.4120, Fax: +1.212.263.4129, fiona.see@nyumc.org. Darren J Kelly, PhD, Department of Medicine, The University of Melbourne, St Vincent's Hospital, 29 Regent Street, Fitzroy, Victoria 3065, Australia, Tel: +61.3.9288.2546, Fax: +61.3.9288.2581, dkelly@medstv.unimelb.edu.au.

DISCLOSURES

Silviu Itescu is Director, Scientific Founder, Chief Scientist, Chairman of Scientific Advisory Board and equity holder of Angioblast Systems, Inc., NY, NY; Director and Chief Scientific Adviser of Mesoblast Ltd, Melbourne, Australia. Michael Schuster is a co-founder and Vice President of Operations of Angioblast Systems, Inc., NY, NY. Henry Krum is a member of the Scientific Advisory Board of Mesoblast Ltd, Melbourne, Australia.

Conclusions—Prospective immunoselection of STRO-3⁺ MPCs from BM MNCs confers advantage in maintaining a population of immature mesenchymal precursor cells during *ex vivo* expansion. Transplantation of culture-expanded MPCs into the post-MI heart results in therapeutic benefit, attributable at least in part to paracrine mechanisms of action. Thus, MPCs represent a promising therapy for myocardial ischemia.

Keywords

cell therapy; adult stem/progenitor cells; paracrine

INTRODUCTION

Mesenchymal stem/progenitor cells (MSCs), derived from adult human bone marrow (BM), represent a leading strategy in the development of cell-based therapies for ischemic heart disease. The salutary effects of MSC administration in animal models of myocardial infarction (MI) include recovery of LV function and attenuation of LV remodeling, associated with augmentation of endogenous cardioprotective processes, such as neovascularization, myocyte survival, and activation of resident cardiac progenitor cells[1–3]. MSC differentiation into cardiomyocyte and endothelial lineage cell types are unlikely to contribute significantly to these therapeutic benefits, given the infrequency of this phenomenon and the typically low engraftment rates of transplanted cells[4–6]. Growing evidence indicates that the cardioprotective and proangiogenic effects of MSC therapy may be attributed, at least in part, to paracrine-based mechanisms of action[7,8]. Clinical application of MSC therapy is favored by the ready availability of source tissue, the ease of isolation and culture-expansion of cells to therapeutically-relevant numbers, and their ability to evade all immune recognition and response[9].

Conventional methods to isolate MSCs from bone marrow (BM) mononuclear cells (MNCs) entail initial selection by plastic-adherence. This approach yields a starting population of cells heterogeneous in morphology, immunophenotype and biological activity, including fibroblastic colony forming unit (CFU-f) and developmental and proliferative efficiencies[10]. Culture-expansion of MSCs is associated with downregulation of stem cell markers, decline of proliferative and differentiation capacities and ultimately cell senescence[11,12]. An alternative approach to MSC isolation involves prospective immunoselection of MSCs on the basis of a common cell surface antigen, with the goal of isolating a more homogenous cell set with respect to biology and function. This strategy may be advantageous in maintaining the population of precursor cells of interest during culture-expansion, and may in turn enhance therapeutic outcome[13]. Antigenic definition of MSCs typically relies upon a panel of surface molecules, including co-expression of CD105, CD73, CD90, and negativity for CD45, CD34, CD14/CD11b, CD79 α /CD19 and HLA-DR, despite these markers being non-specific for MSCs[14,15].

A number of novel candidate markers have been investigated as targets for direct selection of MSCs, including STRO-1, STRO-3, CD49a and VCAM-1[13,16–18]. Growing evidence suggests that STRO-1 marks an immature precursor cell type, which resides in the perivascular niche of human bone marrow[16,19]. STRO-1 expression correlates with various stem cell characteristics including fibroblastic clonogenicity, multipotentiality, telomerase expression and proliferative capacity[11,16]. In the context of myocardial ischemia, STRO-1^{bright} cells may represent a candidate cell type for therapy since intramyocardial delivery of these cells to nude rats post-MI dose-dependently augmented LV functional recovery and arteriolar density, compared to treatment with STRO-1-depleted MNCs[2]. These beneficial effects post-MI may be attributable, at least in part, to soluble factors secreted by STRO-1^{bright} cells since a recent report demonstrated STRO-1

expression to be a determinant for cardioprotective and proangiogenic paracrine activity[13]. Therefore, strategies to select for STRO-1^{bright} cells may represent an important step forward in the development of STRO-1-based therapy.

The recently-described STRO-3 monoclonal antibody, which reacts with a novel epitope of human tissue non-specific alkaline phosphatase, has been shown to identify a subset of STRO-1^{bright} BM MNCs, designated mesenchymal precursor cells (MPCs)[17]. Freshly isolated STRO-1^{bright}/STRO-3⁺ MPCs comprise virtually all CFU-f in BM MNC and demonstrate trilineage developmental potential in *in vitro* and *in vivo* assays[17]. Given the low incidence of MPCs, development of these cells for potential therapy post-MI necessitates culture-expansion to clinically-relevant numbers.

Based on this previous body of work, we hypothesized that culture-expanded MPCs would demonstrate a cardioprotective phenotype. Accordingly, we examined the biological characteristics of culture-expanded MPCs *in vitro*, and we evaluated the therapeutic potential and mechanisms of action of MPCs in a nude rat model of MI.

METHODS

Full details are provided in the Supplementary Methods section.

In vitro biological characterization of MSCs and MPCs

The MNC fraction from human bone marrow aspirates was used to prepare (1) MSC by conventional, plastic-adherence isolation (MSC) [10] and (2) MPC by STRO-3-based prospective immunoselection by magnetic activated cell sorting (MACS) [17]. Following the establishment of CFU-f, passage (P) 0 MSC and MPC were plated as single cell suspensions for *ex vivo* expansion. P4 MSCs and MPCs were compared for: (1) CFU-f efficiency; (2) *in vitro* expansion potential; (3) immunophenotypic profiles and (4) genetic expression of stem cell-related transcripts; and (5) developmental capacities under osteogenic, chondrogenic and adipogenic inductive conditions.

Animal Studies

Supplementary Figure 1 illustrates the 3 animal experiments performed in this study. An athymic nude rat model of MI induced by permanent coronary artery ligation was used in each experiment. In the 14 day MPC study, animals received either MPCs (1×10^6) suspended in saline (N=10) or saline as vehicle control (N=12) by intramyocardial (IM) injection at 48 h post-MI. In the 7 day conditioned medium (CM) studies, animals were treated with IM injections of either concentrated CM derived from 1×10^6 MPCs (P5) cultured in serum-free α MEM (N=12) or control SF- α MEM (N=10) at 48 h post-MI. In the EPC homing study, 1×10^6 human endothelial progenitor cells (EPCs) suspended in saline were delivered by intracardiac injection into the LV of rats at 48 h post-MI. EPCs were allowed to circulate for 15 min prior to intramyocardial injections of CM or control medium (N=12/group).

Cytokine profiling and in vitro biological activity of MPC-CM

Soluble factors present in CM were profiled using a membrane-based antibody array. Concentrations of IL-6, VEGF and MCP-1 were determined using a spectral bead-based immunoassay. The direct effects of CM on neonatal rat cardiac myocytes, human umbilical vein endothelial cells (HUVECs), A7r5 rat vascular smooth muscle cells (rVSMCs) and EPCs were examined in cell culture experiments, in the presence or absence of neutralizing antibodies raised against IL-6, MCP-1 or VEGF.

RESULTS

Biological characterization of STRO-3-immunoselected and culture-expanded MPCs

STRO-3⁺ cells were immunoselected from the MNC fraction of adult human bone marrow aspirate. While CFU-f were detected in unfractionated MNCs, STRO-3-immunoselection resulted in an 8-fold enrichment of CFU-f (Unfractionated *vs.* STRO-3⁺, $P<0.05$). The STRO-3-depleted fraction of MNCs was negative for CFU-f (STRO-3⁺ *vs.* STRO-3⁻, $P<0.05$) (Figure 1A). Cultures of immunoselected STRO-3⁺ MPCs and MSC isolated from MNCs by plastic adherence were expanded up to 9 passages. In comparison to MSCs, population doublings in cultures of STRO-3⁺ MPCs tended to be higher over passages 1–6, and were significantly increased from passages 7–9 ($P<0.05$) (Figure 1B). At passage 4, cell surface expression of STRO-1 and STRO-3 each tended to be higher in MPCs compared with MSCs (Figure 1C). Culture-expanded MPCs demonstrated increased gene expression of a range of stem cell markers, TWIST-1, DERMO-1, Msx2, CBFA-1 and TERT, relative to MSCs (Figure 1D). Levels of transcripts for SDF-1, HGF, IGF-1, VEGF and IL-6, were also elevated in passaged MPCs above MSCs (Figure 1E). Culture-expanded MPCs exhibited a greater capacity to undergo osteogenic ($P<0.05$) (Figure 1F), adipogenic ($P<0.05$) (Figure 1G) and chondrogenic ($P<0.05$) (Figure 1H) differentiation.

Intramyocardial injection of MPCs post-MI in nude rats attenuates LV dysfunction and remodeling

The therapeutic potential of culture-expanded MPCs was examined in a nude rat model of MI. Echocardiographic measurements of fractional shortening (FS) and LV diastolic area (LVAD) obtained at 24 h post-MI indicated that rats randomized to the 2 study groups were well-matched prior to treatment (Figures 2A, 2B). LV function declined following saline injections (–19%, 24 h *vs.* 2 weeks, $P<0.05$) (Figure 2A). In contrast, FS was preserved in MPC-treated rats (+20%, 24 h *vs.* 2 weeks, $P=0.06$) and was higher compared to saline-treated controls at the end of the 2 week study (MPC *vs.* Saline, $P<0.05$). MPC-treatment post-MI also attenuated LV dilatation (+17%, 24 h *vs.* 2 weeks, $P=NS$) compared to saline-treatment (+27%, 24 h *vs.* 2 weeks, $P<0.05$), and resulted in significantly reduced LVAD at the end of the study period (MPC *vs.* Saline, $P<0.05$) (Figure 2B).

At the tissue level, MPC-treated hearts exhibited fewer apoptotic myocyte nuclei at the infarct border compared with saline-treatment ($P<0.05$) (Figure 2C), as well as less extensive areas of fibrosis ($P<0.05$) (Figure 2D) and augmentation of peri-infarct capillary density ($P<0.05$) (Figure 2E).

MPC engraftment in myocardial tissue at 2 weeks following transplantation was examined by immunostaining for human mitochondrial protein. However analysis of stained tissues was confounded by the presence of false positive signals in vehicle-treated MI hearts. These signals were likely attributable to inflammatory cells, given their localization in the infarct region and granular staining pattern (data not shown). As an alternative approach to assessing MPC engraftment, we employed PCR to detect human-specific RPL32 (hRPL32) in DNA extracts from rat MI hearts at 24 h ($N=2$) and 7 d ($N=2$) following intramyocardial injection of MPCs. MPCs were positive for hRPL32, with band intensities corresponding with cell number (Figure 3). DNA from saline-treated rat heart was negative for RPL32. Only weak signals for hRPL32 were detected in MPC-treated hearts at 24 h and 7 d following injection, despite equal loading of samples indicated by comparable levels of rat-specific RPL32. These data indicate rapid loss of MPCs occurs following direct intramyocardial injection at 48 h post-MI.

Intramyocardial injection of MPC-derived CM post-MI preserves LV function and structure, and promotes cardioprotection and neovascularization

We went on to hypothesize that MPC-derived paracrine factors may augment endogenous repair mechanisms in the ischemic heart. MI rats received intramyocardial injections of CM or control medium at 48 h post-MI. FS was similar in both groups prior to treatment, but declined following control medium treatment (-16% , 24 h vs. 1 week, $P<0.05$) (Figure 4A). In contrast LV function was preserved in MI rats treated with CM, such that FS was higher in this group compared to controls at 1 week (CM vs. Control, $P=0.05$). LVAD was also similar in both treatment groups at baseline (Figure 4B). While LVAD increased by 43% in control medium-treated rats (24 h vs. 1 week, $P<0.05$), LV dilatation was attenuated in CM-treated animals ($+26\%$, 24 h vs. 1 week, $P<0.05$), which demonstrated significantly smaller LV cavities at the end of the study ($P<0.05$ vs. Saline).

The benefits of CM on LV function and remodeling over control were associated with reduced myocyte apoptosis in the peri-infarct region ($P<0.05$) (Figure 4C), increased cross-sectional areas of surviving myocytes ($P<0.05$) (Figure 4D) and reduced myocardial fibrosis ($P<0.05$) (Figure 4E).

CM-treatment post-MI also resulted in enhanced myocardial neovascularization, associated with increased proliferation of resident vascular cells compared with control medium. vWF⁺ vessel counts were higher in the peri-infarct region of CM-treated hearts compared with control medium-treated counterparts ($P<0.05$) (Figure 5A). More specifically, CM-treated hearts demonstrated a higher proportion of vWF⁺ vessels co-expressing rat-specific Ki67, a nuclear antigen expressed by proliferating cells, compared with controls ($P<0.05$) (Figure 5B). Intramyocardial injection of CM post-MI also resulted in increases in both the density of α SMA⁺ arterioles in the peri-infarct region ($P<0.05$) (Figure 5C), as well as the proportion of α SMA⁺ vessels co-expressing Ki67 ($P=0.06$) (Figure 5D).

MPC-CM augments EPC mobilization and homing post-MI

To address the question of whether CM promotes EPC mobilization, peripheral blood was collected from MI rats in both treatment groups at the end of the 1 week study period. The concentration of circulating MNCs was increased following intramyocardial CM injection compared to control-medium treatment ($P<0.05$) (Figure 6A). Counts of acLDL⁺lectin⁺ EPCs derived from MNCs of CM-treated MI rats were higher compared with those derived from control-treated counterparts ($P<0.05$) (Figure 6B).

An additional study was undertaken to investigate the effects of CM on EPC homing to the ischemic heart. MI rats received intracardiac injections of DiI⁺ human EPCs, which were allowed to circulate prior to intramyocardial delivery of CM or control medium. At 5 days following injections, DiI⁺ cells were found in the peri-infarct region of myocardial sections taken from both treatment groups. However CM-treated hearts demonstrated significantly higher numbers of DiI⁺ cells compared to control medium-treated hearts (Figure 6C). The increased presence of DiI⁺ cells in CM-treated hearts was associated with increased capillary density ($P<0.05$, vs. Saline) (Figure 6D).

MPC-CM contains cardioprotective and proangiogenic factors

The cytokine profile of CM samples generated under serum-free culture conditions was determined using a membrane-based antibody array system. Detectable signals were semi-quantified by densitometric analysis and expressed relative to control medium (Supplementary Table 1). IL-6, VEGF and MCP-1 were among the factors expressed by MPCs at 2-fold or greater levels above control medium. The concentrations of these factors

were quantified: IL-6: 118.04 ± 0.27 pg/ml; MCP-1: 521.89 ± 1.48 pg/ml; VEGF: 33.95 ± 2.98 pg/ml.

The direct effects of CM on cardiac myocytes were examined *in vitro*. Hypoxic conditions induced apoptosis in myocytes cultured in ischemia-mimetic medium, as indicated by TUNEL (Figure 7A). Myocyte apoptosis was reduced in cells pre-treated with CM+mouse IgG isotype control (CM+mIgG *vs.* Control, $P < 0.05$). This protective effect of CM was partially abrogated by blockade of IL-6 activity (CM+ α IL-6 MAb *vs.* CM+mIgG, $P < 0.05$), though the number of TUNEL⁺ cells in co-treated cultures remained lower than control-treated cells (CM+ α IL-6 MAb *vs.* Control, $P < 0.05$).

CM stimulated hypertrophic growth of myocytes, as evidenced by a marked increase in total cellular protein content, without significant change in DNA content (CM+mIgG *vs.* Control, $P < 0.05$) (Figure 7B). Neutralization of IL-6 attenuated the growth-promoting effect of CM (CM+ α IL-6 MAb *vs.* CM+mIgG, $P < 0.05$). However protein content in myocyte cultures treated with CM+ α IL-6 MAb remained greater than that in control-treated cells (CM+ α IL-6 MAb *vs.* Control, $P < 0.05$). Consistent with these findings, phalloidin-staining of myocytes treated with CM+mIgG for 72 h demonstrated increased size and obvious striation and organization of the contractile protein, actin, into sarcomeric units (Figure 7C). These morphological features were less pronounced in myocytes treated with CM+ α IL-6 MAb.

Cellular proliferation was increased in HUVECs treated with CM+mIgG compared with control medium ($P < 0.05$) (Figure 8A). Blockade of VEGF activity partially inhibited this effect (CM+ α VEGF MAb *vs.* CM+mIgG, $P < 0.05$; CM+ α VEGF MAb *vs.* Control, $P < 0.05$). In comparison to control-treatment, CM stimulated HUVEC migration (CM+mIgG *vs.* Control, $P < 0.05$), which was attenuated by an anti-VEGF antibody (CM+ α VEGF MAb *vs.* CM+mIgG, $P < 0.05$; CM+ α VEGF MAb *vs.* Control, $P < 0.05$) (Figure 8B). CM also promoted HUVEC cord formation on growth factor-reduced Matrigel substrate (Figure 8C and D). Neutralization of VEGF activity in CM disrupted the formation of these cord-like structures (CM+ α VEGF MAb *vs.* CM+mIgG, $P < 0.05$).

CM increased rVSMC proliferation above controls (CM+mIgG *vs.* Control, $P < 0.05$) (Figure 8E). Anti-MCP-1 antibody partially reduced the proliferative effects of CM (CM+ α MCP-1 MAb *vs.* CM+mIgG, $P < 0.05$; CM+ α MCP-1 MAb *vs.* Control, $P < 0.05$). In comparison to control medium, CM stimulated increased rVSMC chemotaxis (CM+mIgG *vs.* Control, $P < 0.05$) (Figure 8F). Inhibition of MCP-1 activity attenuated this chemotactic effect (CM+ α MCP-1 MAb *vs.* CM+mIgG, $P < 0.05$).

EPC proliferation was increased in cultures treated with CM, above levels observed in unstimulated controls (CM+mIgG *vs.* Control, $P < 0.05$) (Figure 9A). Neutralization of VEGF tended to inhibit this effect (CM+mIgG *vs.* CM+ α VEGF MAb, $P < 0.05$). CM also exhibited chemotactic effects on EPCs (CM+mIgG *vs.* Control, $P < 0.05$) (Figure 9B), which were partly attenuated in CM+ α VEGF MAb (CM+ α VEGF MAb *vs.* CM+mIgG, $P < 0.05$; CM+ α VEGF MAb *vs.* Control, $P < 0.05$). CM increased survival of EPCs cultured under hypoxic conditions (CM+mIgG *vs.* Control, $P < 0.05$) (Figure 9C). This protective effect was reduced by blockade of VEGF (CM+ α VEGF MAb *vs.* CM+mIgG, $P < 0.05$). CM stimulated formation of cord-like structures in EPCs grown on Matrigel substrate (Figure 9D). Blockade of VEGF inhibited formation of these structures (CM+ α VEGF MAb *vs.* CM+mIgG, $P < 0.05$).

DISCUSSION

In the present study, we examined the biological characteristics of the culture-expanded progeny of STRO-3-immunoselected MPCs and their therapeutic potential post-MI. The key

findings of this study are: (1) *ex vivo*-grown MPCs exhibited increased proliferative capacity, gene expression for various early stem cell markers and cytokines, and differentiation efficiency compared with conventionally-prepared MSCs; (2) intramyocardial injection of MPCs into rats post-MI attenuated LV dysfunction and remodeling, reduced myocyte apoptosis and augmented myocardial neovascularization, despite poor engraftment of transplanted cells; (3) administration of MPC-CM to the MI heart also mitigated LV dysfunction and dilatation, promoted myocyte survival and hypertrophy and increased vascular density; (4) MPC-CM contained soluble factors with biological activity in cultures of cardiac myocytes, vascular cells, and peripheral blood-derived EPCs.

The recently described STRO-3 monoclonal antibody has previously been shown to enrich for a subset of STRO-1^{bright} MNCs, which is clonogenic and multipotential [17]. Co-expression of high levels of STRO-1 suggest that STRO-3⁺ MPCs may be a relatively immature precursor cell-type with cardioprotective potential[2,16]. The present findings extend on existing data by demonstrating that the culture-expanded progeny of STRO-3-selected MPCs remain proliferative and multipotential following culture expansion over several passages. These functional characteristics were associated with cell-surface expression of STRO-1, and gene expression of a panel of early “stem cell” markers, which are implicated in the regulation of progenitor cell cycle progression and differentiation[12,20–22]. Culture-expanded MPCs also expressed transcripts of various cytokines, reflective of the native function of mesenchymal lineage cells in supporting the population of naïve hematopoietic progenitors in bone marrow. Notably, the proliferative and developmental potentials and stem cell marker and cytokine expression levels were each augmented in cultures initiated by STRO-3⁺ MPCs above that observed in cultures of MSCs established by conventional methods. In sum our data suggest that prospective immunoselection of STRO-3⁺ MPCs enriches for CFU-f, and may be advantageous in maintaining a population of immature mesenchymal precursor cells during culture-expansion, compared with preliminary isolation of MSCs by plastic-adherence alone. Further, these data support the possibility of generating therapeutically-relevant numbers of precursor cells by *ex vivo* expansion for clinical application.

Our *in vivo* studies are the first to demonstrate the cardioprotective and proangiogenic properties of STRO-3-selected and culture-expanded human MPCs in a rat model of MI. Intramyocardial transplantation of 1×10^6 MPCs to rats at 48 h post-MI resulted in improved LV function, reduced dilatation, increased myocyte survival and capillary density associated with reduced fibrosis, compared with saline control at 2 weeks. The dose, route and timing of administration of MPCs were selected based on our previous work, which demonstrated the efficacy of 1×10^6 STRO-1⁺ culture-expanded MPCs in a rat model of MI[2]. The present findings echo our earlier observations of functional recovery and arteriogenesis in the ischemic heart following treatment with STRO-1⁺ MPCs[2]. Similarly, recent reports have demonstrated that in a sheep model of myocardial ischemia, allogeneic-transplantation of STRO-3-selected, *ex vivo*-cultured ovine MPCs attenuated infarct expansion, accompanied by increased vascular density, in a dose-dependent manner, associated with modulation of matrix remodeling[23,24]. Together, these data suggest that the STRO-3 antibody may be employed to select a subset of BM mesenchymal lineage cells, which exhibit a cardioprotective phenotype following culture-expansion.

Interestingly, we found that the beneficial effects of MPC therapy post-MI in rats occurred despite poor engraftment of cells. Specifically, the numbers of MPCs present in the post-MI heart at 24 h and 7 d following injection were dramatically diminished compared to the number injected, and were negligible by 2 weeks. Our observations are similar to reports in the literature of rapid and progressive attrition of MSCs following intramyocardial

transplantation under both syngeneic and xenogeneic conditions[5,25]. In the acute phase post-MI, transplanted cells are likely to be beset by dynamic processes including inflammation, cellular necrosis, fibrosis and metabolic and mechanical disturbances, which may impair engraftment. Our data suggest that under the present study conditions, mechanisms such as MPC differentiation or fusion are unlikely to account significantly for the observed effects of MPC administration post-MI.

Instead, our observations fall in line with a current working hypothesis that the therapeutic benefits observed following MSC administration to the ischemic heart occur, at least in part, via paracrine-mediated mechanisms of action. Various studies have demonstrated beneficial effects of MSC therapy without long-term engraftment, and a link between donor cell-derived factors and LV recovery following MSC transplantation[26–28]. Moreover, injection of MSC-derived factors to the post-MI heart has been shown to rapidly promote angiogenesis and cardioprotection[7,29–31]. Consistent with this body of work, intramyocardial injection of MPC-derived soluble factors post-MI resulted in therapeutic benefits, which mirrored the outcomes observed following treatment of MI rats with MPCs. Profiling of CM revealed the presence of a range of multifunctional soluble factors. Our *in vitro* studies evidence the contribution of IL-6, VEGF and MCP-1 present in CM to its direct actions on myocytes, HUVECs, rVSMCs and EPCs, and suggest possible mechanistic underpinnings for the effects of CM in the post-MI heart. It remains to be determined whether resident cardiac progenitors cells are activated in response to CM treatment, and whether other mechanisms of tissue repair may be involved in the attenuation of LV dysfunction. However, in sum, the present data from our CM studies support the notion that MPCs may exert paracrine-mediated actions when transplanted into the ischemic myocardium.

Interestingly we found that MPC- or CM-treatment post-MI resulted in myocyte hypertrophy both *in vivo* and *in vitro*. Although better function is often coupled with attenuation of myocyte enlargement, hypertrophy of the residual myocardium occurs in the acute phase post-MI as a compensatory response to the loss of tissue at the site of infarct to maintain LV contractile function. Previous studies support the hypothesis that insufficient compensatory hypertrophy post-MI may contribute to LV dilatation and heart failure disease progression[32]. Given the improvements in LV function observed in our study, we speculate that administration of MPCs or CM at 48 h post-MI may augment an early compensatory response, which may contribute to their salutary effects in this context.

Treatment of MI rats with either MPCs or CM also attenuated myocardial fibrosis at the site of infarct. Alongside the concomitant reduction in myocyte apoptosis in the same hearts, our data may suggest that reduced tissue fibrosis in the infarcted region is secondary to augmentation of myocyte survival. In a previous report, the anti-fibrotic and infarct-limiting effects of allogeneic transplantation of STRO-3-derived MPCs into an ovine model of myocardial ischemia were associated with increased indices of collagen degradation[24]. However, the direct actions of MPCs on myocardial collagen turnover remain to be determined. Alternatively, reductions in infarct size and tissue fibrosis following cell therapy in animal models of MI may be attributable to partial regeneration of the necrotic myocardium[33]. In light of poor engraftment of MPCs in the post-MI rat heart, our data support a paracrine mechanism of action for these cells in this setting. However, our data do not preclude the possibility that MPCs may also have the capacity for cardiogenesis, and the potential of MPCs for cardiac development and to activate resident cardiac progenitors or myocytes remains a subject for future investigation.

Our CM studies cast light on a possible paracrine-based mechanism of action of MPC therapy post-MI, though we acknowledge that the data does not provide *direct*

documentation of a paracrine action of MPCs transplanted into the ischemic myocardium. However, our data may provide some insight into the biology of *ex vivo*-grown MPCs. From this perspective, it is important to emphasize that MPC-CM was generated under serum-free and normoxic culture conditions. Thus, our data demonstrate that the constitutive secretome of culture-expanded MPCs includes proangiogenic and cardioprotective factors with biological activity both *in vitro* and *in vivo*. The profile of cytokines identified in this study overlaps qualitatively with that previously detected in MSC-CM, and similarly produced proangiogenic effects in cultures of HUVECs[8]. Interestingly, MPC-CM also promoted myocyte survival under ischemia-mimetic culture conditions and attenuated LV remodeling and dysfunction post-MI, without need for potentiation of MPCs via transfection of survival genes and/or hypoxic culture, which was previously found to be necessary to generate MSC-CM with similar effects[7]. The reasons for these differences in cardioprotective potential between MPC-CM and MSC-CM require further investigation, though we note that in the present study, transcripts for various proangiogenic and cardioprotective cytokines were more abundant in MPCs compared with MSCs prepared by conventional methods. Similarly, Psaltis and colleagues recently reported that CM generated by STRO-1-immunoselected cells demonstrated enhanced cardioprotective and proangiogenic activity compared to MSC-CM[13]. Clearly, the functional consequences of these differences remain to be examined. However, the present data suggest that prospective immunoselection and culture-expansion of STRO-3⁺ MPCs may enrich for a population of cells, which intrinsically expresses a profile of factors that is both qualitatively and quantitatively sufficient to yield therapeutic benefit in myocardial ischemia.

Speculatively, these observations point to the intriguing possibility of MPC-derived soluble factors as therapy *per se*. To this end, the sufficiency of CM generated under serum-free conditions to produce beneficial effects in the ischemic myocardium, and the persistence of these effects at 7 days post-MI, are encouraging. Further investigations might include examination of MPC-CM therapy alone, with animals followed to later time points to determine whether the effects of CM post-MI are sustained. MPC-CM might also be administered in combination with cells types, including EPCs, given the potential synergy between MPC-CM and circulating EPCs observed in this study. In looking ahead toward the possible clinical application of MPCs or CM for post-MI therapy, further efforts are required to optimize these approaches to ensure full exploitation of their respective therapeutic potentials. For example, our data indicate a need for strategies that enhance persistence of MPCs in the ischemic myocardium, since previous studies have shown cell engraftment to correlate positively with therapeutic outcome [34]. Additional experiments, such as a head-to-head comparison of the efficacy of MPC versus CM injections, would also inform evaluation of the most promising way to translate MPC-based therapy for myocardial ischemia into the clinical setting.

The present data support the potential utility of STRO-3 as a marker for a subset of mesenchymal lineage precursors present in adult BM MNCs. Prospective immunoselection of STRO-3⁺ MPCs may be advantageous in maintaining an immature mesenchymal precursor population during *ex vivo* expansion. The culture-expanded progeny of STRO-3⁺ MPCs demonstrated therapeutic potential in the post-MI heart, attributable at least in part, to the secretion of proangiogenic and cardioprotective factors. These characteristics endow MPCs with clinical relevance and promise as therapy for ischemic heart disease.

Supplementary Material

Refer to Web version on PubMed Central for supplementary material.

Acknowledgments

We acknowledge the technical assistance of Geping Zhang.

FUNDING SOURCES

Grant support for this study was provided by the NIH/NHLBI (P50HL077096) and by the Miami Heart Research Institute.

References

1. Amado LC, Saliaris AP, Schuleri KH, et al. Cardiac repair with intramyocardial injection of allogeneic mesenchymal stem cells after myocardial infarction. *Proc Natl Acad Sci USA*. 2005; 102:11474–9. [PubMed: 16061805]
2. Martens TP, See F, Schuster MD, et al. Mesenchymal lineage precursor cells induce vascular network formation in ischemic myocardium. *Nat Clin Pract Cardiovasc Med*. 2006; 3:S18–22. [PubMed: 16501624]
3. Nakanishi C, Yamagishi M, Yamahara K, et al. Activation of cardiac progenitor cells through paracrine effects of mesenchymal stem cells. *Biochem Biophys Res Commun*. 2008; 374:11–6. [PubMed: 18586003]
4. Silva GV, Litovsky S, Assad JA, et al. Mesenchymal stem cells differentiate into an endothelial phenotype, enhance vascular density, and improve heart function in a canine chronic ischemia model. *Circulation*. 2005; 111:150–6. [PubMed: 15642764]
5. Terrovitis J, Stuber M, Youssef A, et al. Magnetic resonance imaging overestimates ferumoxide-labeled stem cell survival after transplantation in the heart. *Circulation*. 2008; 117:1555–62. [PubMed: 18332264]
6. Toma C, Pittenger MF, Cahill KS, et al. Human mesenchymal stem cells differentiate to a cardiomyocyte phenotype in the adult murine heart. *Circulation*. 2002; 105:93–8. [PubMed: 11772882]
7. Gnecci M, He H, Noiseux N, et al. Evidence supporting paracrine hypothesis for Akt-modified mesenchymal stem cell-mediated cardiac protection and functional improvement. *FASEB J*. 2006; 20:661–9. [PubMed: 16581974]
8. Hung SC, Pochampally RR, Chen SC, et al. Angiogenic effects of human multipotent stromal cell conditioned medium activate the PI3K-Akt pathway in hypoxic endothelial cells to inhibit apoptosis, increase survival, and stimulate angiogenesis. *Stem Cells*. 2007; 25:2363–70. [PubMed: 17540857]
9. Aggarwal S, Pittenger MF. Human mesenchymal stem cells modulate allogeneic immune cell responses. *Blood*. 2005; 105:1815–22. [PubMed: 15494428]
10. Pittenger MF, Mackay AM, Beck SC, et al. Multilineage potential of adult human mesenchymal stem cells. *Science*. 1999; 284:143–7. [PubMed: 10102814]
11. Shi S, Gronthos S, Chen S, et al. Bone formation by human postnatal bone marrow stromal stem cells is enhanced by telomerase expression. *Nat Biotechnol*. 2002; 20:587–91. [PubMed: 12042862]
12. Simonsen JL, Rosada C, Serakinci N, et al. Telomerase expression extends the proliferative life-span and maintains the osteogenic potential of human bone marrow stromal cells. *Nat Biotechnol*. 2002; 20:592–6. [PubMed: 12042863]
13. Psaltis PJ, Paton S, See F, et al. Enrichment for STRO-1 expression enhances the cardiovascular paracrine activity of human bone marrow-derived mesenchymal cell populations. *J Cell Physiol*. 2010; 223:530–40. [PubMed: 20162565]
14. Dominici M, Le Blanc K, Mueller I, et al. Minimal criteria for defining multipotent mesenchymal stromal cells. The International Society for Cellular Therapy position statement. *Cytotherapy*. 2006; 8:315–7. [PubMed: 16923606]
15. Sabatini F, Petecchia L, Taviani M, et al. Human bronchial fibroblasts exhibit a mesenchymal stem cell phenotype and multilineage differentiating potentialities. *Lab Invest*. 2005; 85:962–71. [PubMed: 15924148]

16. Gronthos S, Zannettino AC, Hay SJ, et al. Molecular and cellular characterisation of highly purified stromal stem cells derived from human bone marrow. *J Cell Sci.* 2003; 116:1827–35. [PubMed: 12665563]
17. Gronthos S, Fitter S, Diamond P, et al. A novel monoclonal antibody (STRO-3) identifies an isoform of tissue nonspecific alkaline phosphatase expressed by multipotent bone marrow stromal stem cells. *Stem Cells Dev.* 2007; 16:953–63. [PubMed: 18158854]
18. Gindraux F, Selmani Z, Obert L, et al. Human and rodent bone marrow mesenchymal stem cells that express primitive stem cell markers can be directly enriched by using the CD49a molecule. *Cell Tissue Res.* 2007; 327:471–83. [PubMed: 17109120]
19. Shi S, Gronthos S. Perivascular niche of postnatal mesenchymal stem cells in human bone marrow and dental pulp. *J Bone Miner Res.* 2003; 18:696–704. [PubMed: 12674330]
20. Hu G, Lee H, Price SM, et al. Msx homeobox genes inhibit differentiation through upregulation of cyclin D1. *Development.* 2001; 128:2373–84. [PubMed: 11493556]
21. Isenmann S, Arthur A, Zannettino AC, et al. TWIST family of basic Helix-Loop-Helix Transcription Factors Mediate Human Mesenchymal Stromal/Stem Cell Growth and Commitment. *Stem Cells.* 2009; 27:2457–68. [PubMed: 19609939]
22. Shui C, Spelsberg TC, Riggs BL, Khosla S. Changes in Runx2/Cbfa1 expression and activity during osteoblastic differentiation of human bone marrow stromal cells. *J Bone Miner Res.* 2003; 18:213–21. [PubMed: 12568398]
23. Hamamoto H, Gorman JH, Ryan LP, et al. Allogeneic mesenchymal precursor cell therapy to limit remodeling after myocardial infarction: the effect of cell dosage. *Ann Thorac Surg.* 2009; 87:794–801. [PubMed: 19231391]
24. Dixon JA, Gorman RC, Stroud RE, et al. Mesenchymal cell transplantation and myocardial remodeling after myocardial infarction. *Circulation.* 2009; 120:S220–9. [PubMed: 19752372]
25. Muller-Ehmsen J, Krausgrill B, Burst V, et al. Effective engraftment but poor mid-term persistence of mononuclear and mesenchymal bone marrow cells in acute and chronic rat myocardial infarction. *J Mol Cell Cardiol.* 2006; 41:876–84. [PubMed: 16973174]
26. Zhang M, Mal N, Kiedrowski M, et al. SDF-1 expression by mesenchymal stem cells results in trophic support of cardiac myocytes after myocardial infarction. *FASEB J.* 2007; 21:3197–207. [PubMed: 17496162]
27. Iso Y, Spees JL, Serrano C, et al. Multipotent human stromal cells improve cardiac function after myocardial infarction in mice without long-term engraftment. *Biochem Biophys Res Commun.* 2007; 354:700–6. [PubMed: 17257581]
28. Mirotsov M, Zhang Z, Deb A, et al. Secreted frizzled related protein 2 (Sfrp2) is the key Akt-mesenchymal stem cell-released paracrine factor mediating myocardial survival and repair. *Proc Natl Acad Sci USA.* 2007; 104:1643–8. [PubMed: 17251350]
29. Gnecci M, He H, Liang OD, et al. Paracrine action accounts for marked protection of ischemic heart by Akt-modified mesenchymal stem cells. *Nat Med.* 2005; 11:367–8. [PubMed: 15812508]
30. Dai W, Hale SL, Kloner RA. Role of a paracrine action of mesenchymal stem cells in the improvement of left ventricular function after coronary artery occlusion in rats. *Regen Med.* 2007; 2:63–8. [PubMed: 17465776]
31. Timmers L, Lim SK, Arslan F, et al. Reduction of myocardial infarct size by human mesenchymal stem cell conditioned medium. *Stem Cell Res.* 2007; 1:129–37. [PubMed: 19383393]
32. Litwin SE, Raya TE, Anderson PG, et al. Induction of myocardial hypertrophy after coronary ligation in rats decreases ventricular dilatation and improves systolic function. *Circulation.* 1991; 84:1819–27. [PubMed: 1833090]
33. Orlic D, Kajstura J, Chimenti S, et al. Bone marrow cells regenerate infarcted myocardium. *Nature.* 2001; 410:701–5. [PubMed: 11287958]
34. Huang J, Zhang Z, Guo J, et al. Genetic modification of mesenchymal stem cells overexpressing CCR1 increases cell viability, migration, engraftment, and capillary density in the injured myocardium. *Circ Res.* 2010; 106:1753–62. [PubMed: 20378860]

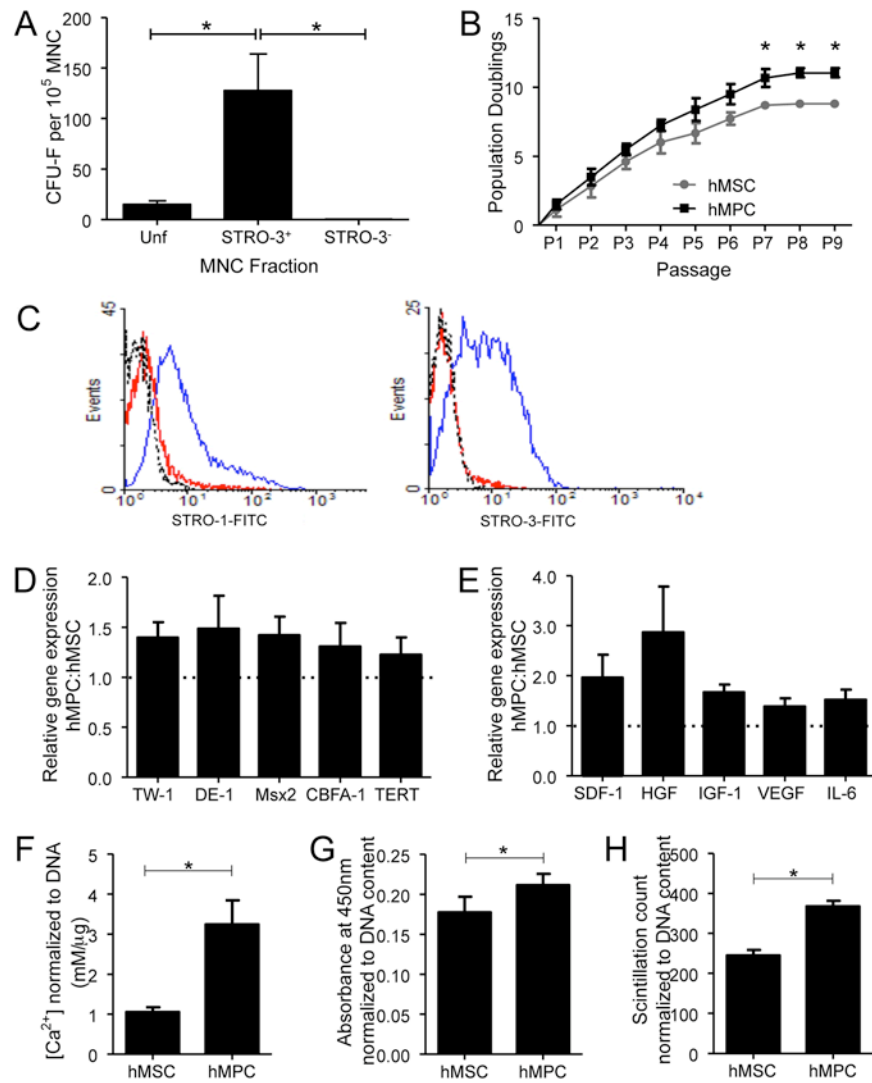


Figure 1. Biological comparisons between MSC and MPC

(A) The clonogenic efficiency of each MNC fraction. Results shown are the mean \pm SEM number of CFU-f per 10^5 cells plated for unfractionated (Unf), STRO-3+ and STRO-3-depleted (STRO-3-) MNC (* P <0.001, average of five donor experiments). (B) Mean number of population doublings (\pm SEM) of MSC and MPC during *ex vivo* culture from P0 to senescence. (* P <0.05, average of 3 donor experiments). (C) Examples of flow cytometric histograms comparing MPC and MSC from the same donor, for surface STRO-1 and STRO-3 expression at P4. Dotted line – isotype control. Red line - MSC. Blue line – MPC. P4 MPC gene expression of various immature “stem cell” markers (D) and cytokines (E). Results are presented as mean ratio \pm SEM of gene expression in MPC relative to MSC (average of three donor experiments). P4 MSC and MPC differentiation capacity for mineralization (F), adipogenesis (G) and glycosaminoglycan synthesis (H), under the respective *in vitro* inductive conditions. Data are presented as mean \pm SEM. (* P <0.05, average of 3 donor experiments.)

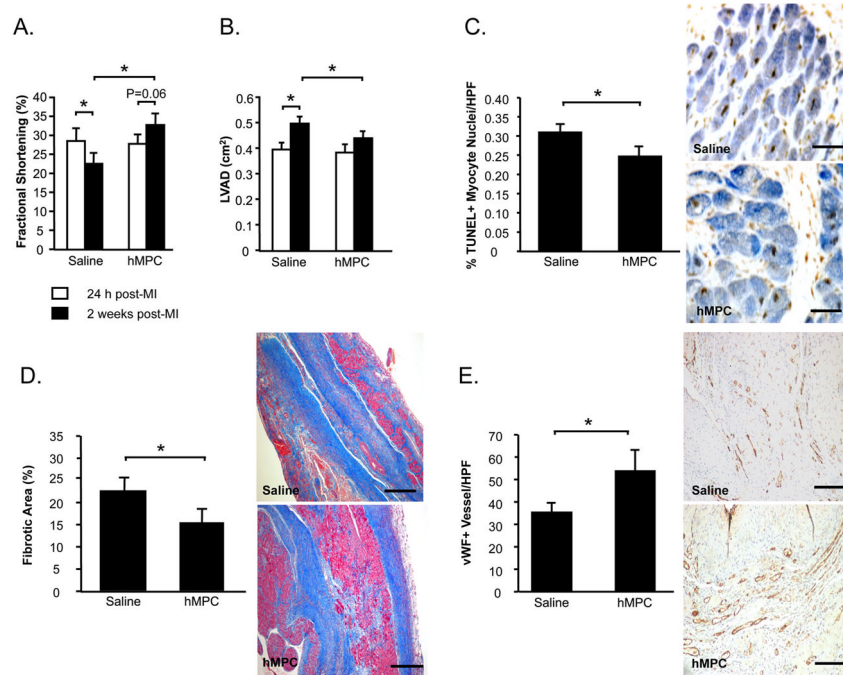


Figure 2. Intramyocardial injection of MPCs post-MI attenuates LV dysfunction and remodeling Echocardiography was performed to assess fractional shortening (A) and LV diastolic areas (LVAD) (B). Myocardial sections were stained to count TUNEL⁺ apoptotic myocytes (C). Masson's Trichrome-stained sections were examined for myocardial fibrosis (D). vWF⁺ vessels per high power field (HPF) were quantified (E). For figures A–E, data is represented as mean±sem. N=10–12/group. *P<0.05.

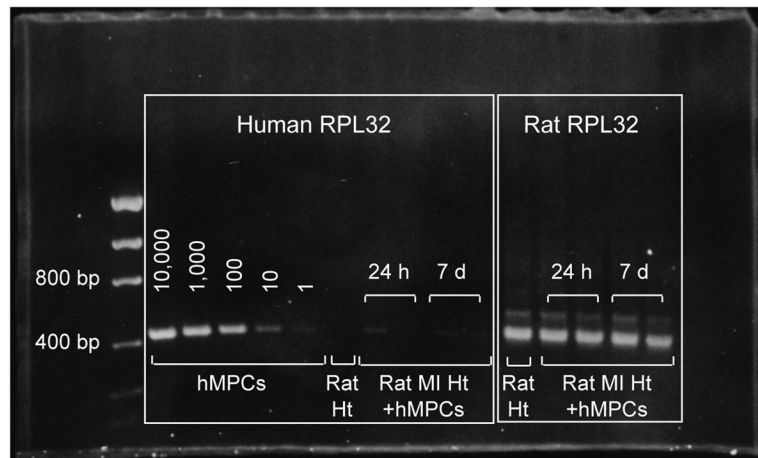


Figure 3. MPCs demonstrate poor engraftment in the ischemic myocardium

Human-specific RPL32 expression (384 bp) in DNA extracts from known numbers of MPCs, untreated control rat heart and human MPC (hMPC)-treated MI hearts harvested at 24 h (N=2) and 7 d (N=2) following intramyocardial injection, was determined by PCR. Rat-specific RPL32 was used as loading control.

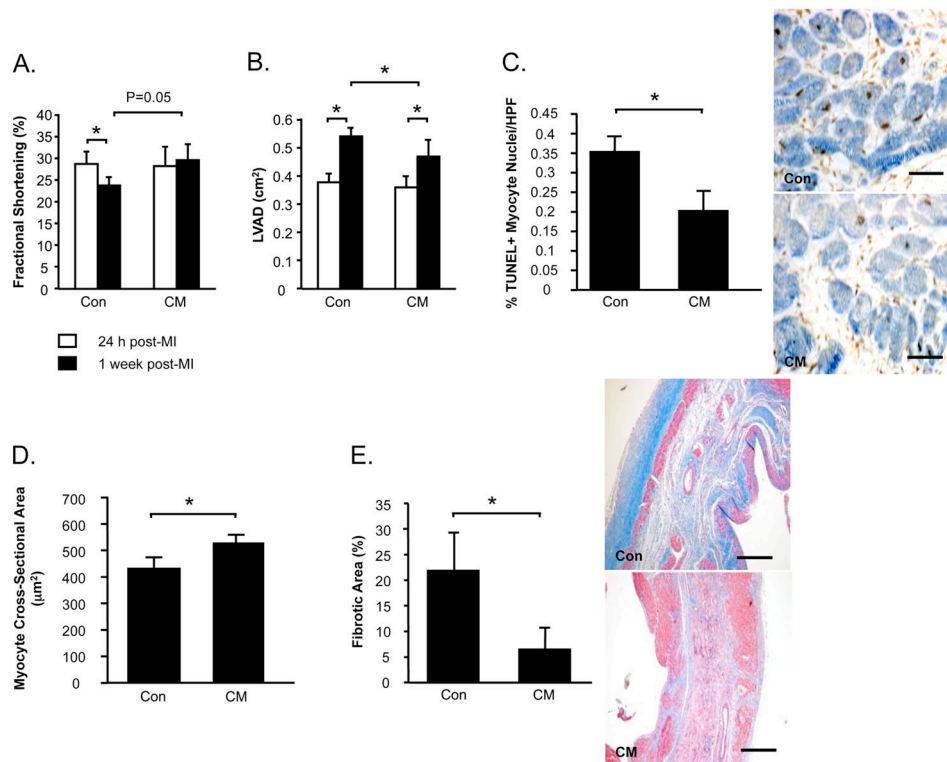


Figure 4. Intramyocardial injection of CM post-MI attenuates LV dysfunction and remodeling Echocardiography was performed to assess fractional shortening (A) and LV diastolic areas (LVAD) (B). Myocardial sections were stained to count TUNEL⁺ apoptotic myocytes (C). Masson's Trichrome-stained sections were assessed for myocyte cross-sectional areas (D) and myocardial fibrosis (E). Data is presented as mean±sem. N=10-12/group. *P<0.05.

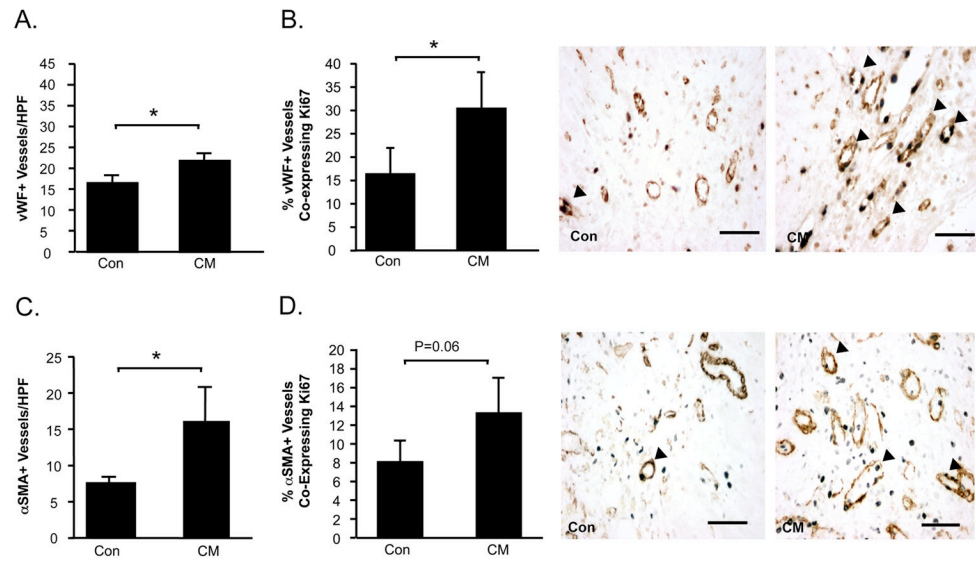


Figure 5. Intramyocardial injection of CM post-MI promotes neovascularization of the ischemic myocardium

Myocardial sections were immunostained to identify capillaries and arterioles. vWF⁺ vessels were counted (A). Proliferating vWF⁺ vessels were identified by co-expression of the proliferating cell nuclear antigen Ki67 (arrow heads) (B). Arterioles were immunostained with αSMA (C). Serial sections were double-stained for αSMA and Ki67 (arrow heads) (D). Data is presented at mean±sem. N=10–12/group. *P<0.05.

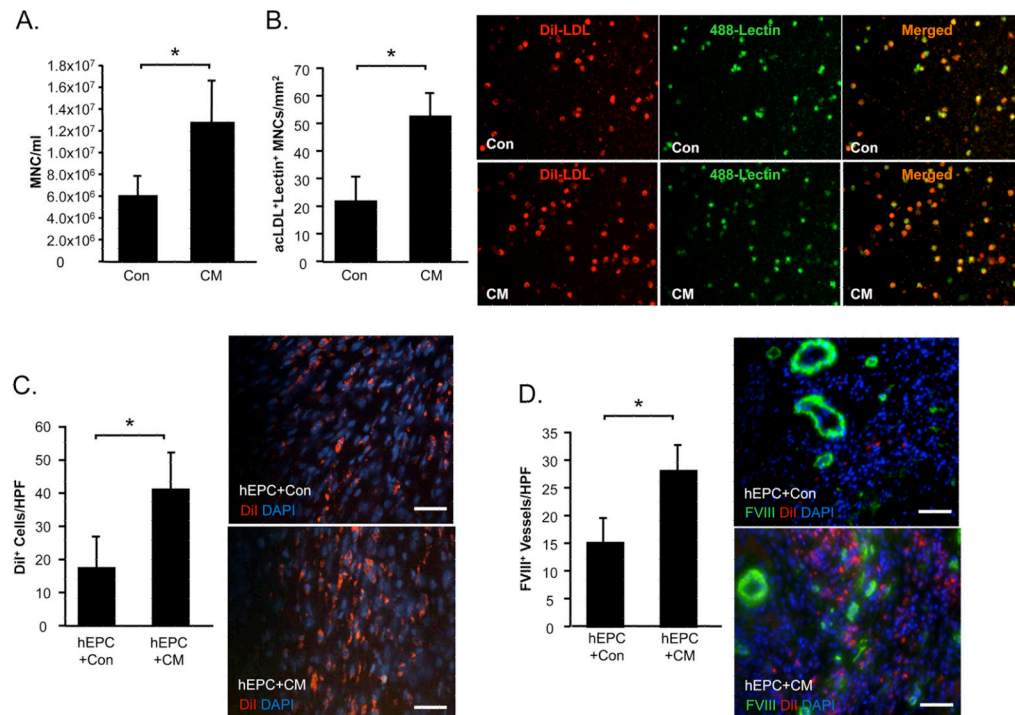


Figure 6. CM augments mobilization and homing of EPCs to the post-MI heart

To examine the effect of CM treatment on EPC mobilization, peripheral blood was sampled from rats at the end of the 1 week study and total MNC were counted (A). acLDL⁺lectin⁺ EPCs cultured from the MNC fraction were counted (B). In a separate experiment, the effects of control medium or CM on DiI⁺ EPCs homing to the ischemic rat heart were examined. At 1 week post-MI myocardial sections were examined for the presence of DiI⁺ cells (C). Myocardial sections were stained to identify vWF⁺ vessels co localized with DiI⁺ EPCs (D). Data is presented at mean±sem. N=10–12/group. *P<0.05.

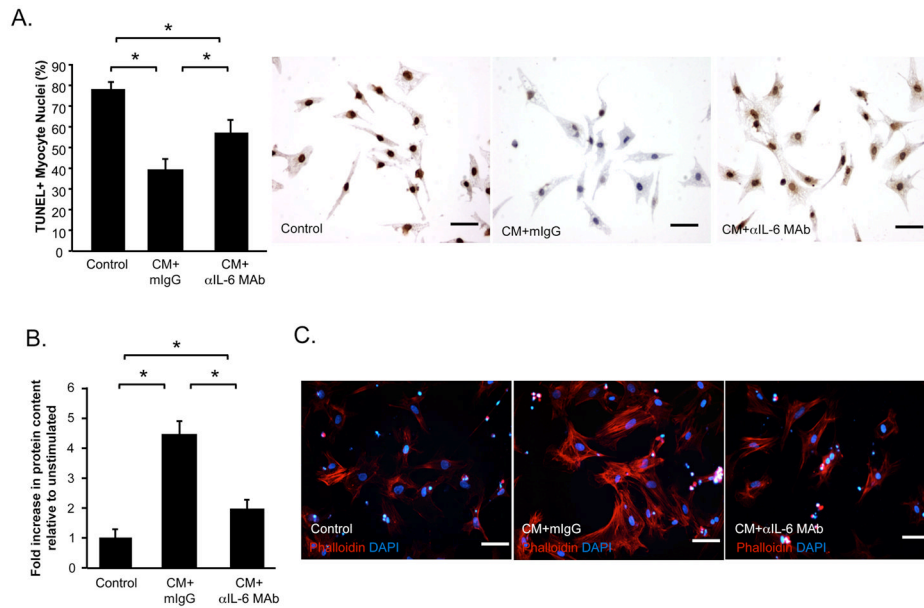


Figure 7. CM protects cardiac myocytes from apoptotic death and promotes myocyte hypertrophy

The direct effects of control medium, CM+mouse IgG isotype control (mIgG) or CM+αIL-6 MAB on neonatal rat cardiac myocytes were examined. (A) Hypoxia-induced apoptosis was determined by TUNEL (brown). Blue: viable nuclei. Myocyte hypertrophy was determined by measuring total protein content, relative to DNA content (B) and phalloidin-staining of fixed cells (C). Data is represented as mean±SEM. Each condition was represented in triplicate. N=3 experiments. *P<0.05.

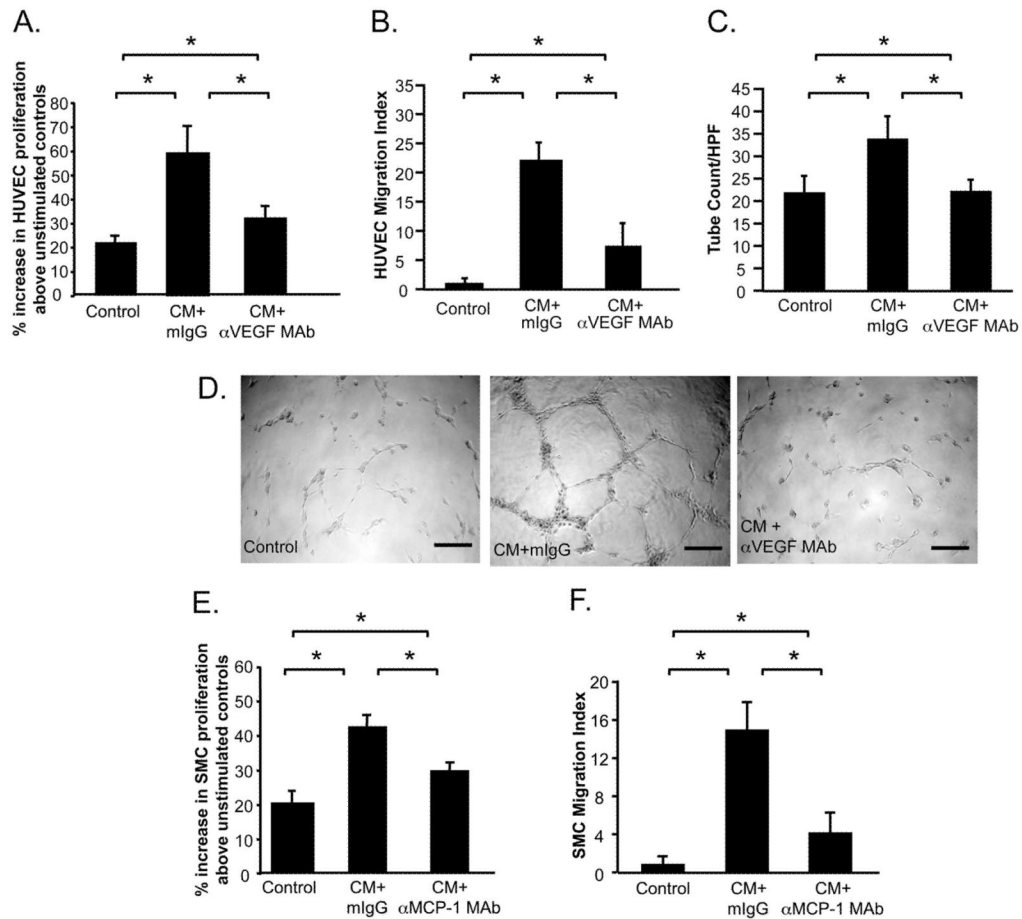


Figure 8. CM promotes vascular cell proliferation, migration, survival and cord formation
 The direct effects of control medium, CM+mouse IgG isotype control (mIgG) or CM + α MCP-1 MAb on cultures of HUVECs were examined in assays for proliferation (A), migration (B) and cord formation (C). Representative images of cord formation in HUVEC cultures (D). The effects of control medium, CM+mouse IgG isotype control (mIgG) or CM + α MCP-1 MAb on rat A7r5 smooth muscle cells were examined with respect to proliferation (E) and migration (F). Data is represented as mean \pm SEM. Each condition was represented in triplicate. N=3 experiments. *P<0.05.

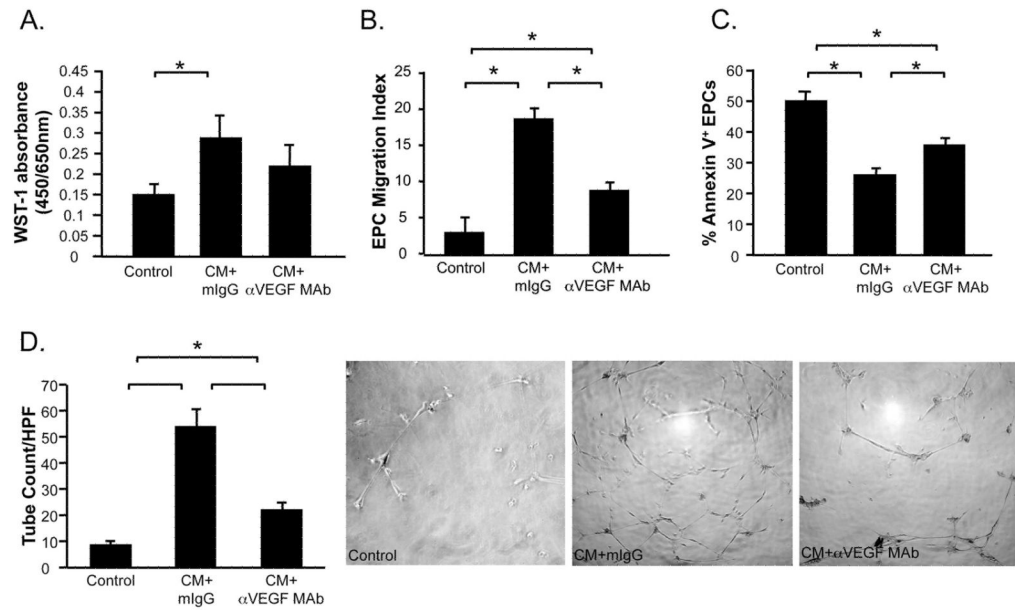


Figure 9. CM promotes EPC proliferation, migration, survival and cord formation

The direct effects of control medium, CM+mouse IgG isotype control (mIgG) or CM +αVEGF MAb on isolated EPCs were examined in assays for proliferation (A), migration (B), apoptosis (C) and cord formation (D). Data is represented as mean±SEM. Each condition was represented in triplicate. N=3 experiments. *P<0.05.